MNRAS **468,** 824–834 (2017)
Advance Access publication 2017 February 24
doi:10.1093/mnras/stx491

The X-ray pulsar 2A 1822−371 as a super-Eddington source

Ann-Sofie Bak Nielsen,[1]★ Alessandro Patruno[1,2]★ and Caroline D'Angelo[1]

[1]*Leiden Observatory, University of Leiden, Niels Bohrweg 2, NL-2333 CA Leiden, the Netherlands*
[2]*ASTRON, the Netherlands Institute for Radio Astronomy, Postbus 2, NL-7900 AA Dwingeloo, the Netherlands*

Accepted 2017 February 21. Received 2017 February 7; in original form 2016 December 17

ABSTRACT

The low-mass X-ray binary 2A 1822−371 is an eclipsing system with an accretion disc corona and with an orbital period of 5.57 h. The primary is a 0.59 s X-ray pulsar with a proposed strong magnetic field of 10^{10}–10^{12} G. In this paper, we study the spin evolution of the pulsar and constrain the geometry of the system. We find that, contrary to previous claims, a thick corona is not required and that the system characteristics could be best explained by a thin accretion outflow due to a super-Eddington mass transfer rate and a geometrically thick inner accretion flow. The orbital, spectral and timing observations can be reconciled in this scenario under the assumption that the mass transfer proceeds on a thermal time-scale that would make 2A 1822−371 a mildly super-Eddington source viewed at high inclination angles. The timing analysis on 13 yr of *Rossi X-ray Timing Explorer* data shows a remarkably stable spin-up that implies that 2A 1822−371 might quickly turn into a millisecond pulsar in the next few thousand years.

Key words: binaries: eclipsing – binaries: general – pulsars: individual: 2A 1822−371 – X-rays: stars.

1 INTRODUCTION

2A 1822−371 is a persistent eclipsing low-mass X-ray binary (LMXB) with a 0.59 s accreting X-ray pulsar (Jonker & van der Klis 2001). The neutron star primary accretes material from a 0.62 $M_\odot$ Roche lobe filling main-sequence star (Harlaftis, Charles & Horne 1997), and the system has a binary orbit of 5.57 h (Hellier et al. 1990; Parmar et al. 2000; Jonker & van der Klis 2001). White et al. (1981) showed that the partial eclipses of the system are best explained by the presence of an accretion disc corona (ADC). The eclipses are clearly seen because the system is being viewed almost edge-on at an inclination angle of 81°–84° (Heinz & Nowak 2001; Jonker, van der Klis & Groot 2003a; Ji et al. 2011), which was found through modelling of the light curve (Heinz & Nowak 2001). As shown by Heinz & Nowak (2001), the eclipse of 2A 1822−371 is a narrow peak in the light curve; however, most of the light curve, about 80 per cent of the orbit, is obscured. White & Holt (1982) suggested that the ADC is formed by evaporated material in the inner accretion disc due to radiation pressure from the X-rays produced by the neutron star. The accretion disc is thought to be optically thick, and the ADC appears so extended that it is not completely blocked by the companion star. Indeed, the companion seems to eclipse about 50 per cent of the total light emitted (Mason & Cordova 1982; Somero et al. 2012). The magnetic field of 2A 1822–371 was inferred twice from the presence of cyclotron resonance scattering features (crsf). Sasano et al. (2014) reported results that was obtained with *Suzaku* and suggested a crsf at 33 keV, which would correspond to a magnetic field of $B \sim 2.8 \times 10^{12}$ G. This, however, was in disagreement with the later findings of Iaria et al. (2015), who interpreted *XMM–Newton* spectral data as showing a crsf at around 0.7 keV (and an inferred magnetic field of $B \sim 8.8 \times 10^{10}$ G).

The intrinsic X-ray luminosity (L_X) of 2A 1822−371 is currently not well constrained. The first source of uncertainty comes from the distance, which is not well known although it was estimated to be around 2–2.5 kpc based on modelling of infrared and optical observations (Mason & Cordova 1982).

Mason & Cordova (1982) estimated the luminosity to be $L_X \sim 1.1 \times 10^{35}\,(d/1\,\mathrm{kpc})$, which for a distance of about 2.5 kpc is $\sim 10^{36}$ erg s^{-1}. Since the pulsar is seen edge-on, its optical to X-ray luminosity ratio is $L_{opt}/L_X \sim 15$–65. This value is very anomalous among LMXBs, which have a typical ratio of the order of ∼1000. The binary also shows a very large orbital period derivative of $\dot{P}_{orb} = 1.5$–2.1×10^{-10} s s^{-1} (implying a very fast orbital expansion; Burderi et al. 2010; Jain, Paul & Dutta 2010; Iaria et al. 2015), and thus, it has been suggested that the binary is undergoing a highly non-conservative mass transfer, with the neutron star accreting at the Eddington limit and the rest of the material expelled from the donor star via radiation pressure (e.g. Iaria et al. 2015). This also suggests the possibility that 2A 1822−371 is an Eddington-limited source (Jonker et al. 2003a), which would then be compatible with one of the magnetic field estimates inferred from the crsf (i.e. $B = 8.8 \times 10^{10}$ G). Another peculiar phenomenon in 2A 1822−371 is the fast spin-up of the system, which gives an extremely short spin-up time-scale of the order of 7000 yr (Jonker & van der Klis 2001). When looking at the ensemble of slow accreting

★ E-mail: nielsen@strw.leidenuniv.nl (A-SBN); patruno@strw.leidenuniv.nl (AP)

pulsars in LMXBs, the short spin-up time-scale of 2A 1822−371 is not unique. Indeed, short time-scales have previously been observed in LMXB pulsars such as 4U 1626−67 and GX 1+4, both of which show torque reversals (Bildsten et al. 1997; Jonker & van der Klis 2001). The accretion torque reversal is a still poorly understood phenomenon that occurs in some accreting pulsars and that causes a switch from a spin-up to a spin-down (and vice versa). One possible interpretation of torque reversals is a transition between a Keplerian and a sub-Keplerian flow in the inner portion of the accretion disc (e.g. Yi, Wheeler & Vishniac 1997).

The spin evolution of 2A 1822−371 can therefore be explained with two different scenarios: either the system has started accreting very recently (if the currently observed spin-up truly represents the secular evolution of the neutron star spin) or, alternatively, what we are observing is simply a short-term effect with the current spin-up that will be possibly balanced by an episode of spin-down in the near future. The latter scenario would make 2A 1822−371 similar to the other high-field LMXB pulsars like 4U 1626−67 and GX 1+4. In those two systems, the phenomenon of torque reversals occurs on time-scales of years. Other pulsars, such as Her X-1, Cen X-3 and Vela X-1 (the latter two are high-mass X-ray binaries), show variations on shorter time-scales of days to a few years (see, for example, fig. 6 in Bildsten et al. 1997). Since several other LMXB pulsars show changes in their spin frequency derivative, we investigate here whether long-term spin-up in 2A 1822−371 is really stable or if there are underlying detectable fluctuations related to accretion torque variations.

A second problem is that, at least in the (low magnetic field) accreting millisecond pulsars, measuring the spin frequency derivative is sometimes complicated by the presence of timing noise in the X-ray time of arrivals (TOAs) of pulsations (Hartman et al. 2008; Patruno, Wijnands & van der Klis 2009). It has, however, been observed that at least in some accreting millisecond pulsars, a large part of timing noise is correlated to variations in flux (Patruno et al. 2009, 2010; Haskell & Patruno 2011). One plausible interpretation of the flux–phase correlation is that the hotspot is moving on the pulsar surface in response to variations of the mass accretion rate. In high-field accreting pulsars like 2A 1822−371, the presence of such correlation has never been reported and it is currently unclear whether such effects might be present in these systems too. For example, the stronger magnetic field of the neutron star in 2A 1822−371 might prevent a drift of the hotspot when the accretion rate varies. However, strong timing noise has been observed in the accreting X-ray pulsar Terzan 5 X−2 (Patruno et al. 2012), which is an 11 Hz accreting pulsar with a magnetic field of the order of 10^9–10^{10} G, which is substantially stronger than the typical field observed in accreting millisecond pulsars ($B \sim 10^8$ G). Therefore, it might be possible that the same phenomenon is present in 2A 1822−371, and in this work, we plan to investigate this. Therefore, there are two questions that need to be addressed for 2A 1822−371:

(1) Is the previously measured spin frequency derivative the true one or is its measurement affected by the presence of timing noise?
(2) Does the (true) spin frequency derivative represent the long-term spin evolution of the neutron star?

In this paper, we use archival data from the *Rossi X-ray Timing Explorer* (*RXTE*), collected over a baseline of 13 yr, to try to answer the aforementioned questions.

Furthermore, it has been suggested that the ADC forms an optically thick region around the neutron star (White & Holt 1982; Parmar et al. 2000; Iaria et al. 2001), with optical depth $\tau \sim 9$–26, which implies that most of the light coming from the pulsar is heavily scattered. However, at such large optical depths, the coherent pulsations cannot preserve their coherence. Iaria et al. (2013) first noticed this problem and suggested that the Comptonized component is produced in the inner regions of the system, which are never directly observed. Then, only a small fraction (∼1 per cent) of the total light produced is scattered along the line of sight of the observer with an optical depth $\tau \sim 0.01$. This geometry, although possible, requires some fine tuning of the optical depth. Furthermore, to preserve the coherence of the pulsations, the whole (optically thick) Comptonization region needs to rotate with the neutron star. A third question that needs to be answered is therefore whether it is possible to keep a simple geometry of the system, with an ADC, and still obtain a spectrum compatible with $\tau \sim 1$.

In Section 2, we present the observations and the data reduction procedure; in Section 3, we show our results on the timing analysis, e.g. the spin evolution and flux–phase correlation; and in Section 4, we discuss the implications of our finding and we extend previous models for 2A 1822−371 .

2 X-RAY OBSERVATIONS

We have used data taken over a baseline of 13 yr between 1998 June 28 and 2011 November 30. All observations were taken with the Proportional Counter Array (PCA) on board the *RXTE* (Bradt, Rothschild & Swank 1993; Jonker & van der Klis 2001). *RXTE*/PCA consists of five xenon/methane proportional counter units, which are sensitive in the range of 2–60 keV (Jahoda et al. 2006). We chose science event files with a time resolution of 2^{-16} s (Event_16us), 2^{-13} s (Event_125us) and 2^{-20} s (GoodXenon) for the timing analysis, whereas we selected Standard 2 data with 16 s time resolution to construct the X-ray light curve. The light curve is reconstructed in the 2–16 keV energy range and the X-ray flux is first averaged for each observation (ObsID) and then normalized in Crab units (see Fig. 4). A detailed description of this standard procedure can be found in van Straaten, van der Klis & Méndez (2003). The timing analysis is performed by selecting the absolute energy channels 24–67 that correspond approximately to an energy range of ≈9–23 keV. This range was chosen because the pulsation has the highest signal-to-noise ratio (S/N) as reported by Jonker & van der Klis (2001). The data were barycentred with the FTOOL *faxbary* by using the JPL DE405 Solar system coordinates and the most precise astrometric position found by *Chandra* observations, RA: $18^{\rm h}25^{\rm m}46\overset{\rm s}{.}81$ and Dec: $-37^\circ06'18\overset{''}{.}5$ (Burderi et al. 2010) with an error of 0.6 arcsec (90 per cent uncertainty circle of the *Chandra* X-ray absolute position). The barycentred data were then epoch folded in pulse profiles of 32 bins over either 1500 s, or the total length of the data segment, which usually corresponds to 3000 s. We then cross-correlated each pulsation with a sinusoid at the spin frequency of the pulsar and generated a set of TOAs. We selected only pulsations with an S/N larger than 3.1σ, defined as the ratio between the pulse amplitude and its 1σ statistical error. The value of 3.1σ is selected to account for the number of trials, that is, we expect less than 1 false pulse detection among the 281 pulse profiles generated over the entire 13 yr baseline. We looked for the presence of a second harmonic that was detected only in a small subset of data segments, and thus we do not consider it any further in the forthcoming timing analysis.

The ephemeris used in the epoch folding are composed by an initial pulse frequency from Jonker & van der Klis (2001) and Jain et al. (2010) and an orbital solution from Iaria et al. (2011). The orbital solution corresponds to a Keplerian circular orbit with a constant orbital period derivative. Since the data contain large data

Table 1. Overview of the data used throughout this paper. The data are taken with *RXTE*, and in this data, segments 3, 9, 10, 13, 14 and 15 represent data not analysed before in the literature (Jonker & van der Klis 2001; Jain et al. 2010; Somero et al. 2012). The errors reported in the parentheses correspond to 1σ statistical errors. The χ^2 and degrees of freedom given in the table is for the TEMPO2 spin frequency fit to the data. The 95 per cent upper confidence limit is only given for the data segments, where no significant pulsations were found (significance limit was 3.3σ).

# segment	ObsId	$T_{\rm start}$	$T_{\rm end}$	Upper limit (per cent)	PEPOCH	Spin frequency (ν_0)	Spin period ($P_{\rm s}$)	χ^2	dof
1	30060	50 992.8210	50 993.9805		50 993.1873	1.686 0862(6)	0.593 089 49(2)	28.49	6
2	30060	51 018.2434	51 019.6464		51 018.9449	1.686 0957(3)	0.593 086 15(9)	63.30	17
3	50048	52 031.5426	52 032.8178		52 032.1105	1.686 6984(4)	0.592 8742(3)	35.43	13
4	50048	52 091.4522	52 101.4647		52 096.4049	1.686 7365(2)	0.592 860 83(7)	47.41	12
5	70036	52 435.4107	52 435.7670		52 435.5174	1.686 932(2)	0.592 792 12(5)	25.54	8
6	70037	52 488.3701	52 495.9115		52 491.9201	1.686 971 04(4)	0.592 7784(2)	100.13	26
7	70037	52 503.3513	52 503.9363		52 503.5256	1.686 980(2)	0.592 775 26(5)	21.77	8
8	70037	52 519.1659	52 519.5110		52 519.3091	1.686 988(4)	0.592 772 44(1)	42.79	6
9	70037	52 547.3079	52 547.8544		52 547.3944	1.687 0063(10)	0.592 766 01(4)	26.31	9
10	70037	52 608.1849	52 608.3845		52 608.2072	1.686 879(8)	0.592 810 75(3)	11.22	2
11	70037	52 882.0214	52 882.2226		52 882.3290	1.687 240(4)	0.592 683 91(2)	8.81	3
12	70037	52 883.1514	52 885.1249		52 883.4896	1.686 9901(8)	0.592 771 71(3)	20.55	2
13	80105	52 896.2822	52 896.4384		52 896.2556	1.687 243(3)	0.592 682 86(9)	11.12	4
14	96344	55 880.6677	55 884.8487		55 882.5852	1.689 1897(2)	0.591 999 82(6)	85.27	17
15	96344	55 888.5020	55 895.6318		55 891.8696	1.689 20448(8)	0.591 994 64(3)	23.85	7
16	60042	52 138.7535	52 141.8115	2.1	–	–	–	–	–
17	60042	52 138.7535	52 141.8115	2.1	–	–	–	–	–
18	50048	51 975.7203	51 976.1843	0.7	–	–	–	–	–
19	70037	52 432.3887	52 432.7906	0.6	–	–	–	–	–
20	70037	52 724.7351	52 724.7545	0.5	–	–	–	–	–

gaps, we split it in 20 segments that could be potentially phase connected, meaning that our time baseline for each different segment spans typically a few days (see Table 1). With the S/N criterion discussed above, we found significant pulsations in 15 out of 20 data segments. In this work, we have used TEMPO2 version 2012.6.1 and kept the orbital values fixed throughout the analysis.

3 RESULTS

Pulsations are found in the first 15 data segments described in Table 1. In the last five data segments, the S/N found was lower than the selected 3.1σ for most of the pulsations, thus leaving us with too few or no pulsations to perform the timing analysis. In Table 1, we provide the 95 per cent confidence upper limit of the fractional amplitude of the pulsations in these five data segments. All these upper limits are consistent with the fractional amplitude found in the first 15 data segments.

3.1 Spin evolution

In 2 out of 15 data segments, the pulse TOAs of the neutron star required a spin frequency derivative. The χ^2 and degrees of freedom (dof) for the fits to all 15 data segments are given in Table 1. The errors on the spin frequency were calculated by using standard χ^2 minimization techniques and by multiplying them by the square root of the reduced χ^2. The errors on the spin period are found from $\sigma_{\rm P} = \sigma_\nu(\frac{1}{\nu})^2$.

The collection of all spin frequencies (see Table 1) is then fitted with a linear function to determine the long-term spin frequency derivative over the entire baseline of the observations. The fit gives a reduced χ^2 of 1909 for 11 dof. This indicates that the fit is not statistically acceptable (p-value < 0.05 per cent) and the bad fit is caused by several points that are clearly off the linear relation (see the lower panel of Fig. 1). The best-fitting linear slope that we find corresponds to a spin-up of $\dot{\nu} = 7.6(8) \times 10^{-12}$ Hz s^{-1} for the period

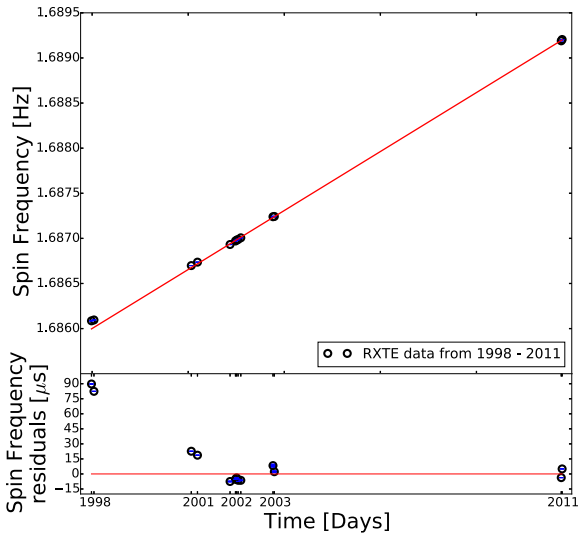

Figure 1. The long-term spin-up over a time period of 13 yr. The black points show the data used in this paper and listed in Table 1. The red line is a fit to the data from this paper and it gives the spin-up of the pulsar of $\dot{\nu} = 7.57(6) \times 10^{-12}$ Hz s^{-1}. This figure is plotted with errors on all points, seen in blue. Most of the errors are, however, so small that they are not visible on the plot.

ranging from 1998 June to 2011 November, comparable to what has recently been found by Chou et al. (2016).

The bad fit to the spin frequencies shows that, although there is no evidence for a change in sign of the spin frequency derivative, some fluctuations are present in the data. We thus explored to what extent the magnitude of the accretion torque varies with time and whether *small/short-term* torque reversals are present in the data. First, in the data segments 4 and 6, it was possible to phase-connect the pulsations and we thus have a direct measure of the spin frequency derivative. Such spin frequency derivative is measured for a time

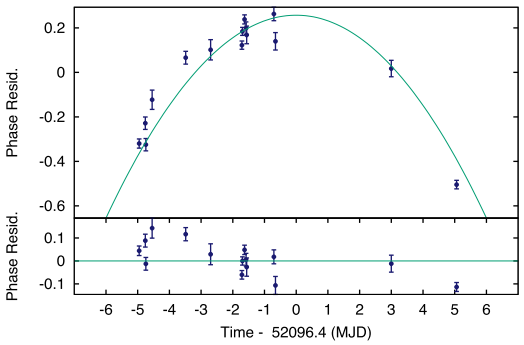

Figure 2. The pulse phase residuals before a spin frequency derivative is fitted for (top panel) and after (lower panel). The parabola is a clear evidence of the presence of a spin frequency derivative.

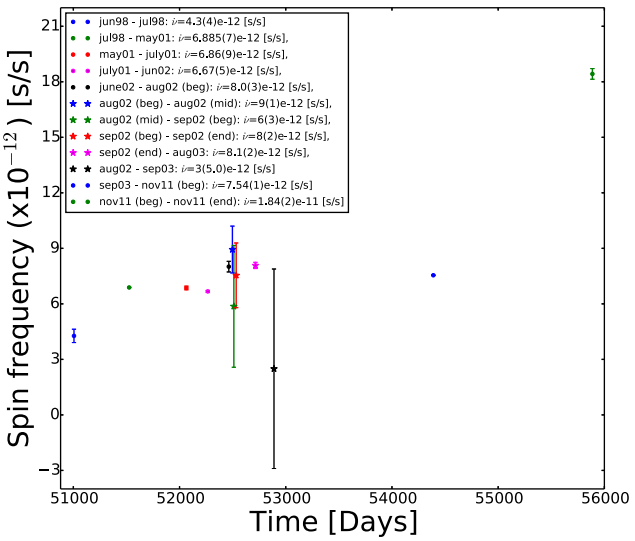

Figure 3. The spin period derivative change between the individual observations from Fig. 1. It is clearly seen that most of the observations coincide, and there is a close to constant development in the spin period derivative. However, there are a few points that are off, e.g., in 2003 and 2011.

interval of 10 and 8 d (for segment 4 and 6, respectively). The two spin-up values found are $\dot{\nu} = 6.7(4) \times 10^{-12}$ Hz s^{-1} for segment 4 and $\dot{\nu} = 8.2(5) \times 10^{-12}$ Hz s^{-1} for segment 6, which are both within 1σ from the long-term linear trend seen in the 13-yr long baseline.

The pulse phase residuals with respect to a constant spin frequency model can be seen for the data segment 4 in the top panel of Fig. 2. In the lower panel of the same figure, we show the pulse phase residuals with respect to a spin frequency derivative model. The parabolic trend seen in the top panel of Fig. 2 is a clear signature of the presence of a frequency derivative.

3.2 Spin period derivative versus time

To estimate the magnitude of the spin fluctuations, we calculated the spin period derivative between each consecutive data point; that is, we determined the slope between each pair of points, and plotted them versus time, see Fig. 3. The errors on the spin period derivatives are found by taking the maximum and minimum slope between the spin periods in Fig. 1. It is clear that most of the points in Fig. 3 are roughly consistent with a single constant spin period derivative with small variation of less than a factor of 2 over the whole baseline with the exception of an outlier in the last data segment taken in 2011.

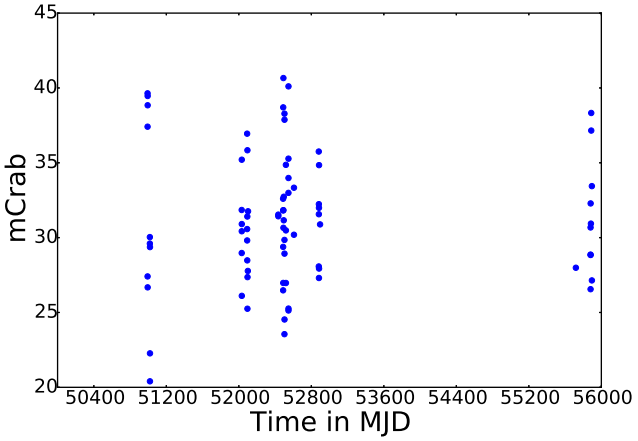

Figure 4. 2–16 keV X-ray light curve of 2A 1822−371. Each data point represents an ObsID average flux. The overall intensity of the light curve is fairly constant over the span of the observations used in this paper, with variations of less than a factor of 2 in 13 yr of observations.

In that case, the spin frequency derivative is consistent with having increased by a factor of 3 during the last month of the observations.

The 2–16 keV X-ray flux shows a variation of less than a factor of 2 during that same month (see Fig. 4) and no average variation when compared to the average X-ray luminosity of the previous years.

3.3 X-ray flux–phase correlation

2A 1822−371 is a persistent source that shows little variability in X-ray flux. In all our observations, the X-ray flux varies by less than a factor of 2 with respect to the average value. Therefore, even if a flux–phase correlation is present in 2A 1822−371, we expect little or no variation in the X-ray pulse phases. None-the-less, we inspected the data for the presence of such correlation, since it is the first time that such a test is performed in such a high-field accreting pulsar.

We follow the procedure outlined in Patruno et al. (2009, 2010); that is, we minimize the χ^2 of a linear fit to the X-ray flux versus pulse phase. If there is a significant correlation, then this might indicate the existence of some mechanism that determines the pulse phase variations in addition to genuine neutron star spin variations. Such mechanism, for example, can be the motion of the hotspot on the surface of the pulsar (Patruno et al. 2009, 2010).

We fit the data with a linear correlation

$$\phi = a + b\, F_{\rm X}, \qquad (1)$$

where ϕ is the pulse phase and $F_{\rm X}$ is the the X-ray flux. If there is a correlation, b should be significantly different than zero. However, in all our 15 data segments, the b coefficient is consistent with zero within the statistical errors as can be seen in Table 2.

3.4 Fractional amplitude versus cycles

We tested whether there was a correlation between the fractional amplitude of the pulsations and the eclipses with the purpose of testing whether we can actually directly see the surface of the neutron star when there is no eclipse.

In Fig. 5, we report the results of the data analysed from 2002 and 2011. The fractional amplitude definition is the same as the one used in Patruno et al. (2010). When pulsations are not detected, we

Table 2. The a and b values for the flux–phase correlation fits for the individual data segments.

# segment	a	b
1	−0.08(10)	0.001(2)
2	0.20(3)	−0.0087(7)
3	0.2(1)	−0.007(4)
4	0.81(6)	−0.03(2)
5	0.08(7)	−0.003(2)
6	0.004(40)	−0.0001(15)
7	0.19(5)	−0.008(2)
8	−0.22(5)	0.010(2)
9	0.12(5)	−0.005(2)
10	−0.5(1)	0.019(4)
11	−1.8(2)	0.080(7)
12	0.11(8)	−0.004(3)
13	0.4(1)	−0.012(3)
14	−0.07(5)	0.002(2)
15	−1.20(7)	0.033(2)

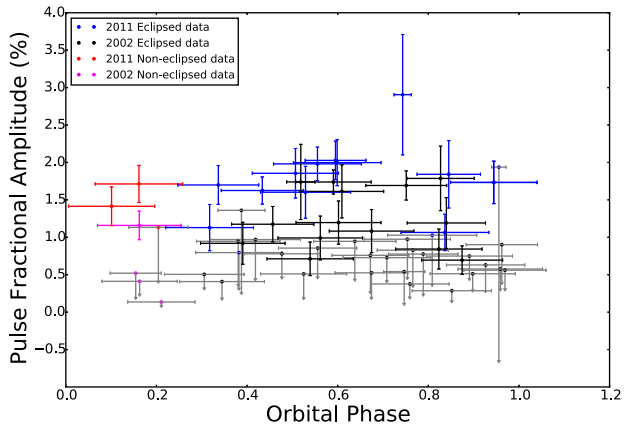

Figure 5. The fractional amplitude of eclipsed data and the non-eclipsed data versus the cycle of the pulsar. The eclipse fractional amplitudes are seen in blue/green (2011 and 2002 data), and the non-eclipsed fractional amplitudes are seen in red/pink (2011 and 2002). The non-eclipsed data are assumed to be 0.05–0.25 cycle, and the rest of the cycle is assumed to be a part of the eclipse. The eclipse is defined with a zero-point at $T_{\rm ASC}$.

provide 95 per cent confidence level upper limits. The red and pink points in Fig. 5 are the data from the non-eclipsed part of the light curve, and the blue and black points are from the eclipsed part of the orbit. We use $T_{\rm asc}$ as our reference orbital phase zero (i.e. the beginning of the cycle) and we thus expect that the non-eclipsed data are between cycle 0.05 and 0.25. We further use the fact that the rest of the cycle is partially eclipsed. Note that some other authors use a different definition of eclipse; for example, Heinz & Nowak (2001) define the eclipse to be only the portion of the light curve that shows a deep dip (Hellier et al. 1990; Heinz & Nowak 2001). In any case, Fig. 5 shows that there is no detectable difference between the fractional amplitudes for the eclipsed and non-eclipsed data in any orbital phase interval.

4 DISCUSSION

In this paper, we have found a long-term spin frequency derivative of $\dot{\nu} = 7.6(8) \times 10^{-12}$ Hz s^{-1} and a short-term spin frequency derivative of $\dot{\nu} = (6–8) \times 10^{-12}$ Hz s^{-1} in two phase-connected data segments. The long-term spin-up is consistent with that reported by Chou et al. (2016), Iaria et al. (2015), Jain et al. (2010) and Jonker & van der Klis (2001). We have found no evidence for torque reversals and few variations in the accretion torque, limited to fluctuations of less than a factor of 2 with the exception of the last data segment in 2011, where the spin-up requires an increase by a factor of 3 with respect to the overall long-term spin frequency derivative. There is no corresponding increase in the X-ray flux (in the 2–16 keV band) at the time of the spin-up increase. Finally, no evidence for a phase–flux correlation and no strong variations in the X-ray flux of the source are found.

Previous papers have suggested different models and parameters for 2A 1822–371. A summary of some of the most recent papers is found in Table 3. The data examined in this paper span a baseline of about 13 yr from 1998 to 2011. In the following sections, we will try to explain the long-term spin evolution with a self-consistent model that can explain the measured strength of the magnetic field, the neutron star spin frequency derivative and the mass transfer rate. Then we will move on to comment on the different possible magnetic fields reported by Iaria et al. (2015) and Sasano et al. (2014). We then proceed to discuss whether the observed spin frequency derivative reflects a secular spin-up that will continue in the future, or whether we are indeed just observing a short-term spin-up that will change sign and/or magnitude in the future.

4.1 Long-term spin evolution

The large spin-up of 2A 1822−371 implies a very short spin-up time-scale of about $\nu/\dot{\nu} \approx 7000$ yr. This is an extremely short time-scale for a system that should take several million years to spin-up (Bhattacharya & van den Heuvel 1991). The relatively constant spin-up implies no variation in the accretion torques acting upon the neutron star at least down to time-scales of 8–10 d. However, as shown in Section 3.1, the linear fit to the spin frequency versus time gives a very large χ^2, which implies that the spin frequency is not increasing linearly with time. This would be expected in case of constant accretion torque, but the observed flux has a root mean square (rms) fluctuation of the order of 4.4 mCrab, suggesting that accretion torques do indeed vary slightly with time. The strongest evidence for this comes from the last data point in 2011 where the spin-up increases by a factor of 3. Accretion theory predicts that the strength of the spin-up should scale with the amount of mass accreted according to the following relation (see e.g. Bildsten et al. 1997):

$$\dot{\nu} \propto \dot{M}^{6/7}. \tag{2}$$

If the mass accretion rate is related to the X-ray luminosity (and thus the X-ray flux) with the usual relation $L_{\rm X} \approx \eta\, c^2 \dot{M}$, then we should expect $\dot{\nu} \propto F_{\rm X}^{6/7}$. Therefore, a three times larger $\dot{\nu}$ should imply an ≈3 × larger X-ray flux. However, the average 2–16 keV X-ray flux is not varying, on average, by this amount and therefore this probably means that the 2–16 keV X-ray flux is not a good tracer of the instantaneous mass accretion rate. Such possibility has been proposed to explain the behaviour of a number of other LMXBs (van der Klis 2001).

We now wish to test if we can find a self-consistent model that explains the observed spin parameters of 2A 1822−371. First, let us define the corotation radius as that point in the accretion disc where matter has the same angular velocity of the neutron star:

$$R_{\rm CO} = \left(\frac{G M_{\rm NS}}{4\pi^2 \nu^2}\right)^{1/3}. \tag{3}$$

Table 3. The different parameters in the most recent published papers on 2A 1822−371. The papers are JvdK2001 = Jonker & van der Klis (2001), Jain2010 = Jain et al. (2010), Bay2010 = Bayless et al. (2010), Sas2014 = Sasano et al. (2014) and Ia2015 = Iaria et al. (2015).

Parameter	JvdK2001	Jain2010	Bay2010(UV/Optical)	Sas2014	Ia2015
$\dot{\nu}$ (Hz s^{-1})	$(8.1 \pm 0.1) \times 10^{-12}$	$(7.06 \pm 0.01) \times 10^{-12}$	–	$(6.9 \pm 0.1) \times 10^{-12}$	$(7.25 \pm 0.08) \times 10^{-12}$
$\dot{P}_{\rm Spin}$ (s s^{-1})	$-2.85(4) \times 10^{-12}$	$-2.481(4) \times 10^{-12}$	–	$-2.43(5) \times 10^{-12}$	$-2.55(3) \times 10^{-12}$
$L_{\rm X}$ (erg s^{-1})	10^{36}–10^{38}	$(2.38$–$2.96) \times 10^{38}$	$\sim 10^{37}$	$\sim 10^{37}$	1.26×10^{38}
$\dot{M}$(M$_\odot$ yr^{-1})	–	$(4.2$–$5.2) \times 10^{-8}$	6.4×10^{-8}	–	–
$M_{\rm NS}$(M$_\odot$)	1.4	1.4	1.35	1.4	1.61–2.32
B (G)	10^{8}–10^{16}	$(1$-$3) \times 10^{8}$	–	2.8×10^{12}	$8.8(3) \times 10^{10}$
Pulse amp	0.25–3 per cent	–	–	$\sim \pm 5$ per cent	$\sim$0.75 per cent
$P_{\rm orb}/\dot{P}_{\rm orb}$ (yr)	–	$(4.9 \pm 1.1) \times 10^{6}$	$(3.0 \pm 0.3) \times 10^{6}$	–	–
$P_{\rm s}$ (s)	0.593 25(2)	0.592 6852(21)	–	0.592 437(1)	0.592 8850(6)
Time span	1996–1998	1998–2007	1979–2006	2006	1996–2006

Then, following Ghosh & Lamb (1979), we can define the magnetospheric radius as the point where the ram pressure of the disc plasma equals the magnetic pressure:

$$R_{\rm m} = \xi R_{\rm A} = \xi \left(\frac{\mu^4}{2GM_{\rm NS}\dot{M}^2} \right)^{1/7}. \quad (4)$$

Such definition has some issues, since it is derived by equating the dipolar magnetic field pressure to the ram pressure of a spherically symmetric free-falling gas. The factor $\xi \approx 0.5$ is typically used to account for the disc geometry instead of the spherical symmetry of the free-falling gas. Several works (Aly 1985; Lovelace, Romanova & Bisnovatyi-Kogan 1995; Goodson, Winglee & Böhm 1997) have demonstrated that the magnetospheric-disc interaction will quickly generate an azimuthal field component that causes many field lines to open and reconnect at infinity. D'Angelo & Spruit (2010, 2012) have thus derived a different version of the magnetospheric radius that accounts for this difference. The magnetospheric radius thus obtained, however, is not substantially different from the expression above, and since we are giving only an order of magnitude estimate of the quantities, we will continue to use the definition above. This also makes the comparison with other works more direct, since they mostly rely on the definition of magnetospheric radius given by Ghosh & Lamb (1979).

From Table 3, we can see that a few parameters reported in the literature (e.g. B, L_X, $\dot{P}_{\rm s}$, etc.) are not consistent with each other and sometimes some reported values are even inconsistent from a physical point of view. For example, magnetic field strengths as large as 10^{16} G have been discussed by Jonker & van der Klis (2001), by using the relation between B and μ, which, can only be used when $R_{\rm m} < R_{\rm CO}$, since there will be no accretion if the magnetospheric radius is outside of the corotation radius (with the exception of accretion induced by magnetic diffusivity, see e.g. Ustyugova et al. 2006). For 2A 1822−371, the corotation radius is at $\approx$1200 km, so that any magnetospheric radius larger than this value cannot be inferred by using equation (3). With a B field of 10^{16} G, one would indeed obtain a magnetospheric radius of 10^{6} km for a luminosity of 10^{36} erg s^{-1}.

Since we know $\dot{\nu}$, we can use the relation for the X-ray luminosity to find the mass accretion rate ($\dot{M}$) (Frank, King & Raine 2002):

$$\dot{M} = \frac{L_{\rm X} R_{\rm NS}}{G M_{\rm NS}}. \quad (5)$$

This assumes that the X-ray luminosity does trace the instantaneous mass accretion rate, which is, however, not the case in 2A 1822−371, as we have shown above. To obtain an expression for μ that we have used in equation (4), we use the angular acceleration as a function of $\dot{M}$, $\dot{\Omega} = 2\pi\dot{\nu} = \frac{M\sqrt{GM_{\rm NS}R_{\rm m}}}{I}$ that gives

$$\dot{\nu} \approx 4.1 \times 10^{-5} \dot{M} M_{\rm NS}^{1/2} R_{\rm m}^{1/2} I^{-1} {\rm Hz\,s^{-1}}. \quad (6)$$

In the above equation, we use the measured long-term $\dot{\nu}$, and we assume a neutron star mass of 1.4 M$_\odot$, a neutron star radius of 10 km, the moment of inertia ($I = 10^{45}$ g cm^2, $\xi = 0.5$). We assume 1.4 M$_\odot$ in the above text, even though Iaria et al. (2015) find the mass of the neutron star to be (1.69 ± 0.13) M$_\odot$ and find the companion mass to be (0.46 ± 0.02) M$_\odot$, within the limits given by Muñoz-Darias, Casares & Martínez-Pais (2005).

We can see that the models that satisfy the condition $R_{\rm m} < R_{\rm CO}$ are those where the luminosity is in excess of the Eddington limit. However, it is not known if the star really does accrete near the Eddington limit. The observed X-ray luminosity is only $L_{\rm X} \approx 10^{36}(d_2)^2$ erg s^{-1}, assuming a (poorly constrained) distance of 2 kpc. The best distance approximation is between 1 and 5 kpc (Mason & Cordova 1982; Parmar et al. 2000); that, however, would shift the luminosity by less than an order of magnitude. The most compelling evidence that the X-ray luminosity is indeed higher than the observed value is that the ratio $L_{\rm X}/L_{\rm opt} \approx$ 15–65 and not 500–1000 as observed in other LMXBs (Griffiths et al. 1978; Bayless et al. 2010; Somero et al. 2012; Iaria et al. 2015). This means that either the optical luminosity is much larger than expected or that only a small amount (1–10 per cent) of the total X-ray luminosity of the source is effectively observed.

A source accreting at the Eddington rate requires a mass accretion rate of $\dot{M} \sim 10^{-8}$ M$_\odot$ yr^{-1}. This is two orders of magnitude larger than what is expected from binary evolution models under the assumption that the donor is a main-sequence star that started Roche lobe overflow with a mass $\lesssim$1 M$_\odot$ and that the binary evolution is driven by angular momentum loss via magnetic braking (Podsiadlowski, Rappaport & Pfahl 2002). Since 2A 1822−371 is a persistent source, the mass accretion rate (from the disc to the neutron star) must be equal to (or very close to) the mass transfer rate (from the donor to the accretion disc). Therefore, in this model the system will only survive for about 1 Myr.

It is interesting to compare the behaviour of 2A 1822−371 with that of Terzan 5 X−2, another pulsar that is in many ways similar to 2A 1822−371. Terzan 5 X−2 is an 11 Hz accreting pulsar that is accreting from a sub-giant companion ($M \gtrsim 0.4$ M$_\odot$) in a relatively large orbit (orbital period of 21 h). The neutron star has a dipolar magnetic moment in the range of $\mu \simeq 10^{27}$–10^{28} G cm^3 (Cavecchi et al. 2011; Papitto et al. 2011; Patruno et al. 2012). This system has a clear spin-up of $\dot{\nu} \sim 10^{-12}$ Hz s^{-1}, and it appears to be evolving towards a millisecond pulsar in a very short time-scale of a few

tens of million years (Patruno et al. 2012). Both 2A 1822−371 and Terzan 5 X−2 seem to be at odds with the very long phases that binaries with similar spin and orbital parameters spend in Roche lobe contact, which can last for about 1 Gyr or more. Patruno et al. (2012) proposed that Terzan 5 X−2 is in an exceptionally early Roche-lobe overflow (RLOF) phase although the reason why we are witnessing this unlikely event remains an open problem. Indeed, observing two pulsars being recycled in an early RLOF phase in the relatively small population of LMXBs is unlikely. This means that the exceptionality of Terzan 5 X−2 cannot be due to chance alone and there must be a common evolutionary process that creates this kind of accreting pulsars. By using the proper motion, the radial velocity and the current position of 2A 1822−371, it is possible to find the original position and give an estimate of the age of the system. Maccarone, Girard & Casetti-Dinescu (2014) found 2A 1822−371 to likely originate from close to the Galactic centre, and reported an age of about 3–4 Myr, which indeed makes the system very young (Maccarone et al. 2014, although there is quite a big uncertainty due to the poorly constrained distance of the system). This may support the analogy that the system is similar to Terzan 5 X−2 and they are both in an early Roche lobe overflow phase.

4.2 Torque reversal

2A 1822−371 shares a few common features with other accreting pulsars, besides Terzan 5 X−2. Short spin-up time-scales are also seen in the ultracompact binary 4U 1626−67 (Chakrabarty et al. 1997) which has $\nu/\dot{\nu} = 5000$ yr (Chakrabarty et al. 1997; Beri et al. 2014). 4U 1626−67 is a quite different binary from 2A 1822−371, since it is an ultracompact system ($P_{\rm orb} \approx 42$ min), the companion star is not a main-sequence star, but rather a degenerate He or CO white dwarf, and the neutron star has a spin of 7.66 s. The system was originally discovered in 1972 by Giacconi et al. (1972). Torque reversal of the system was observed for the first time in 1990, where the system was found to be spinning down rather than up, as previously observed (Chakrabarty et al. 1997; Beri et al. 2014).

The torque reversal phenomenon is not very well understood, since it is unclear what its origin is and what triggers it. However, the accretion torque in 4U 1626−67, no matter the sign of the spin frequency derivative, is very steady on time-scales of years, which means that the accretion is almost certainly from an accretion disc. Chakrabarty et al. (1997) even found that the pulsar seems to be accreting steadily during spin-down. The first phase of spin-up lasted for at least 13 yr, the spin-down then lasted about 18 yr, and in 2008 4U 1626−67 began spinning up again (Beri et al. 2014). In 4U 1626−67, the torque reversals are accompanied by sudden variations in the X-ray luminosity (Chakrabarty et al. 1997). A decrease in X-ray flux was seen when the neutron star moved from a spin-up to a spin-down phase, and again there was an increase by a factor of 2 in the X-ray flux with the second torque reversal (Beri et al. 2014). The very short spin-up time-scale found for 2A 1822−371 is thus not incompatible with the notion that this system too will show a torque reversal somewhere in the near future.

4.3 Accretion disc corona

From the spectral analysis of 2A 1822−371 and from the shape of the eclipses, it is evident that there is some extended X-ray emitting region around the pulsar, often assumed to be the ADC, that scatters the light originating on the pulsar (White & Holt 1982; Heinz & Nowak 2001; Iaria et al. 2013).

One possible scenario is that an extended Comptonizing region is in fact the accretion curtain as it falls towards the neutron star, and it is possible that the emission we see is actually produced by photons upscattered through this curtain. To investigate this more quantitatively, we build a toy model for the spectrum, in which the underlying emission from the star (which we assume to consist of a blackbody and Comptonized hard X-ray component) is upscattered by hot electrons in the infalling accretion curtain. We use the method and code of D'Angelo et al. (2008) to produce the final Compton upscattered spectrum. We start with an initial input spectrum (assumed originating from the stellar surface) of a blackbody plus an additional power-law component with a cut-off at high energies. We then use this as a seed photon spectrum to generate an output spectrum as a result of inverse-Compton upscattering through a hot (e.g. $\gtrsim$10 keV) thermal electron cloud.

To model this process, we use a Monte Carlo Compton scattering code, whose details are described in Giannios & Spruit (2004). Briefly, the code works by using the seed photon spectrum as the initial photon energy distribution, and then calculating the outcome (final photon energy and direction) of a seed photon inverse-Compton scattering off a hot electron. The electron cloud energy distribution is assumed to be thermal, and the temperature of the cloud is an input parameter of the simulation. The cloud is assumed to be isotropically surrounding the source of seed photons, and the probability of scattering depends mainly on the optical depth of the electron cloud (another input parameter).

The model thus has six free parameters, four for the input spectrum: the blackbody temperature ($t_{\rm bb}$), the power-law slope (Γ) and cut-off energy ($E_{\rm c}$), the relative strength of the blackbody to power law (N) and two for the Comptonizing cloud: its temperature ($T_{\rm e}$) and optical depth (τ). We vary these parameters in order to explore the range of temperatures and optical depths for the electron cloud that could be made consistent with the observed X-ray spectrum.

The requirement of an ADC has been introduced in the literature to explain the excess of light seen during the eclipses, with the X-ray flux never reaching a value of zero as expected from a full eclipse. The X-ray flux is seen hovering at around 50 per cent of its non-eclipse value. Furthermore, the very long duration of the partial eclipses (about 80 per cent of the orbit) requires an extended source surrounding the central X-ray source (White & Holt 1982; Hellier et al. 1990). The ADC was suggested to be formed from evaporated material in the accretion disc (White & Holt 1982). Shakura & Sunyaev (1973) suggested that the central source of X-ray binaries could evaporate material from the disc, and that if the material does not escape the system, it could form a corona-like cloud around the central source. White & Holt (1982) showed that the central source is always obscured if the inclination angle of the system is more than 60°, which is compatible with what is observed for 2A 1822−371, with an inclination angle of $i = 82.^{\circ}5 \pm 1.^{\circ}5$ (Heinz & Nowak 2001). As we have shown in Section 3.4, this scenario is compatible with the behaviour of the pulsed fraction as a function of the orbital phase. Indeed, the fractional amplitude of the pulsations is consistent with being constant regardless of the orbital phase of the binary. This implies that the neutron star is obscured by some material throughout the orbit. Another important point is that the fractional amplitude of the pulsar does not vary with the depth of the eclipses. This does support the idea that the surface of the neutron star is never observed and that the pulsations we do see are indeed scattered through some medium, e.g. an ADC or an accretion stream.

Iaria et al. (2015, 2001) and Parmar et al. (2000) previously suggested that the ADC must be optically thick. This was also discussed

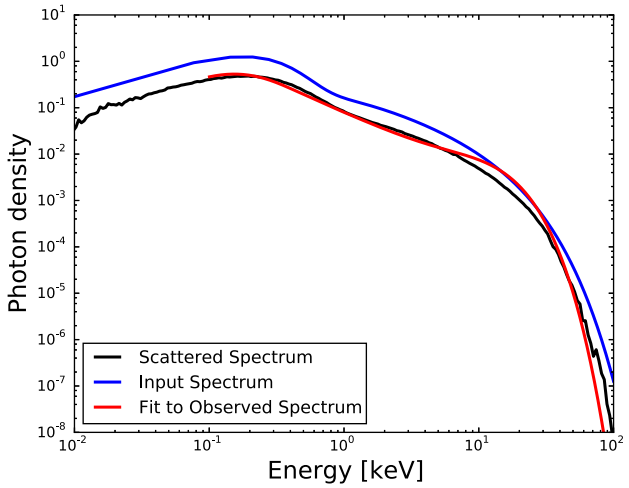

Figure 6. The blue line represents the best simulated spectrum. The blue line is our guess corresponding to the red line, which is the fit to the spectrum of X 1822−371 used by Iaria et al. (2015). The green line is the input spectrum we have used, consisting of both a blackbody and a power-law component.

by Heinz & Nowak (2001) and Iaria et al. (2013), who stated that an optically thick ADC is not consistent with the pulsations observed. To explore the possibilities for a lower value for the optical depth, we explored the parameter space for the optical depth, the power-law index and the electron temperature of the Compton upscattering cloud. We found it possible to create an input spectrum, which, sent through the Compton upscattering cloud, would be similar to the fitted spectrum with a high optical depth used by Iaria et al. (2015). This can be seen in Fig. 6, where the red line is the fit used by Iaria et al. (2015), the blue line is the input spectrum we created, using both a power law and a blackbody, and the black line is the output spectrum after the input spectrum has been sent through a Compton cloud.

The blue line in Fig. 6 corresponds to a power-law index of $\Gamma = 1$, electron temperature of $E_c = 10$ keV and optical depth of $\tau = 1$. Our test of the optical depth should be taken only as a proof of principle, that a model spectra with a blackbody and a power law can recreate the spectra observed *even if the optical depth is small*. The quality of the spectra and its match with the spectra found, for example, by Iaria et al. (2015) is judged by eye and by the normalized rms deviation that we find to be 28 per cent.

The limits for the electron temperature is $3 < T_e < 15$ keV, the power-law index limits are $0.5 < \Gamma < 1.5$ and the acceptable range of optical depth is $0.01 < \tau < 3$. Within these limits, the spectra are reasonably reproduced with a much lower optical depth that is thus compatible with the presence of pulsation without the requirement of an optically thick Comptonization region plus an optically thick scattering ADC, as suggested in Iaria et al. (2013). These results are also compatible with recent spectral modelling performed by Niu et al. (2016), which discussed the possibility that the ADC around 2A 1822−371 is indeed optically thin.

The fit we created gives a simple structure of the system, where the ADC is surrounding the pulsar, and reaching further out than the secondary star, making the pulsar light coming from an extended source, and thus both explaining the pulsations and the 50 per cent depth of the eclipses. The structure of the system we suggest is initially very simple when compared to what White & Holt (1982) suggested. By analysing a spectrum that consists of both a power law and a blackbody component, it is possible to eliminate the optically thick Comptonizing region, and thus explain the system only with an optically thin (or moderately thick; $\tau \approx 0.01$–3) ADC surrounding the pulsar. Another possibility for the geometry is that we could be seeing this system through an extended accretion stream. This stream scatters the light and pulsations just as an ADC would do. Assuming this as an explanation, simplifies the structure of the system even further.

2A 1822−371 is not the only suggested ADC system. Another such system is MS 1603.3+2600. MS 1603.3+2600 was discovered by Morris et al. (1990) and has a 1.7 h orbital period (Jonker et al. 2003b). The source shows both similarities and differences with 2A 1822−371. Both sources appear to be at a fairly high inclination, although the precise value for the inclination angle is not known for MS 1603.3+2600. MS 1603.3+2600 is thought to be at a distance of about 6–24 kpc (Parmar et al. 2000; Jonker et al. 2003b; Hakala et al. 2005). Despite not showing accretion-powered pulsations, MS 1603.3+2600 has a neutron star primary, since the source shows type I X-ray bursts (Jonker et al. 2003b; Hakala et al. 2005). The existence of an ADC around the source is supported by variations in the X-ray bursts. Hakala et al. (2005) looked at two *XMM–Newton* observations taken on 2003 January 20 and 22. They observed several type I X-ray burst candidates. The bursts during the first observation have a count rate of about 6 counts s^{-1}, whereas those seen during the second part of the observation only have a count rate of 2–3 counts s^{-1}. The variation suggests that the bursts are not directly observed; thus, it is possibly only scattered X-rays that are observed, with the scattering medium forming an ADC (Hakala et al. 2005).

4.4 2A 1822−371 as a super-Eddington source

A big weakness of the model that we have discussed so far is that it requires an Eddington-limited accretion rate, despite the binary containing a low-mass main-sequence star that should transfer mass at a rate of about 10^{-10} $M_\odot$ yr^{-1}. Jonker et al. (2003a) performed detailed optical observations of 2A 1822−371 and suggested that one possible interpretation of the spectroscopic results is that the donor star is out of thermal equilibrium. Cowley et al. (2003) also suggested that the donor must be somewhat evolved since otherwise it would not fill its Roche lobe. Muñoz-Darias et al. (2005) also proposed that 2A 1822−371 is an LMXB which descends from an intermediate-mass X-ray binary progenitor (initial $M \gtrsim 1\,M_\odot$), with the companion that has already lost a substantial amount of mass. In this case, the mass transfer would not be driven by angular momentum loss via magnetic braking and/or gravitational radiation but would proceed on the thermal (Kelvin–Helmotz, KH) time-scale of the companion (see e.g. King et al. 1996).

The thermal time-scale is $\tau_{KH} \approx G M_2^2/(2\,R\,L_{nucl})$, where G is the universal gravitational constant, M_2 is the companion mass, R_2 is its radius and L_{nucl} is the nuclear stellar luminosity. The stellar luminosity is not well known in 2A 1822−371, since the optical observations are usually dominated by the disc emission/irradiation. Furthermore, as shown by King et al. (1995), the thermal time-scale changes when irradiation is present, since the stellar surface luminosity might exceed the nuclear luminosity. Since the observed X-ray luminosity is of the order of 10^{36} erg s^{-1} and assuming that all the irradiation luminosity is re-emitted by the stellar surface of the donor, the irradiation luminosity would, due to geometric effects, correspond to approximately 10^{34} erg s^{-1} and the KH time-scale becomes $\tau_{KH} \gtrsim 10^7$ yr, using $M_2 = 0.46\,M_\odot$ and R_2 corresponding to the Roche lobe radius, $R_L = 0.6\,R_\odot$. If the companion star

evolved on the $\tau_{\rm KH}$ time-scale, then the mass transfer rate can be as high as $\sim 10^{-7}\,{\rm M}_{\odot}\,{\rm yr}^{-1}$.

We now try to interpret the observations of 2A 1822−371 in light of this hypothesis. In the following, there is a big uncertainty on most parameters, thus the results could vary within an order of magnitude, and are only approximate. The orbital separation of 2A 1822−371 changes for two reasons: (1) the redistribution of angular momentum in the binary and (2) the loss of angular momentum via magnetic braking/gravitational wave emission (see e.g. Frank et al. 2002):

$$\frac{\dot{a}}{a} = \frac{2\dot{J}}{J} + \frac{-2\dot{M}_2}{M_2}(1-q), \tag{7}$$

where $q = M_2/M_{\rm NS}$ is the mass ratio between the companion (M_2) and neutron star mass ($M_{\rm NS}$), a is the orbital separation, J is the angular momentum and the dot refers to the first time derivative. In J we include all effects, e.g. magnetic breaking, gravitational waves and mass-loss (Tauris & van den Heuvel 2006). If the mass transfer $\dot{M}_2 \approx 10^{-7}\,{\rm M}_{\odot}\,{\rm yr}^{-1}$ then, assuming to first order a conservative mass transfer scenario ($\dot{J} \approx 0$), we expect a relative variation of the orbit $\dot{a}/a \sim 10^{-14}\,{\rm s}^{-1}$. The observations of the orbital period derivative $\dot{P}_{\rm orb} \approx 1.51 \times 10^{-10}$ (Iaria et al. 2011) provide a direct test of this hypothesis. Indeed from the third Kepler law, we expect that $\dot{a}/a = 2\,\dot{P}_{\rm orb}/3\,P_{\rm orb}$ and the observed values give $2\,\dot{P}_{\rm orb}/3\,P_{\rm orb} \approx 5 \times 10^{-15}\,{\rm s}^{-1}$, which is in good agreement with the hypothesis that 2A 1822−371 is evolving on a thermal time-scale in a conservative mass transfer scenario.

Since the mass transfer is super-Eddington, we can follow the line of reasoning of King & Lasota (2016), where they examine the case of the ultraluminous X-ray source M82 X−1. If that donor in M82 X−1 is in a super-Eddington mass transfer phase then the mass accretion rate, magnetic radius and the magnetic moment of the neutron star (μ) can be inferred from first principles. We argue here that one remarkable possibility to explain the phenomenology of 2A 1822−371 is that it is a mildly super-Eddington source.

In this case, the accretion disc will be the standard Shakura–Sunyaev geometrically thin disc down to the so-called spherization radius (Shakura & Sunyaev 1973):

$$R_{\rm sph} = \frac{27}{4}\frac{\dot{M}_{\rm tr}}{\dot{M}_{\rm Edd}} R_{\rm g}, \tag{8}$$

where $\dot{M}_{\rm tr}$ and $\dot{M}_{\rm Edd}$ are the mass transfer rate ($10^{-7}\,{\rm M}_{\odot}\,{\rm yr}^{-1}$) and the Eddington limit for a neutron star (that we set equal to $\approx 2 \times 10^{-8}\,{\rm M}_{\odot}\,{\rm yr}^{-1}$) and $R_{\rm g} = GM/c^2 \approx 2 \times 10^5$ cm is the neutron star gravitational radius ($M_1 = 1.69\,{\rm M}_{\odot}$). This gives a spherization radius of $\sim 10^7$ cm. Beyond this radius, the flow will become geometrically thick and generate a funnel flow that can produce beaming (see e.g. King 2009).

If the innermost region of the accretion disc is truncated at the magnetospheric radius $R_{\rm M}$, with $R_{\rm M} < R_{\rm sph}$, then the local mass accretion rate in any annulus of the disc with radius $R < R_{\rm sph}$ needs to be

$$\dot{M}(R) = R/R_{\rm M}\dot{M}_{\rm Edd}. \tag{9}$$

Together with the expression for the magnetic dipole moment and spin-up (equation 6), the spherization radius and the mass accretion rate equations (equations 8 and 9) form a set of four equations with four variables, $R_{\rm sph}$, $\dot{M}(R_{\rm M})$, μ and $R_{\rm M}$. Following the method by King & Lasota (2016), one finds $R_{\rm M} \sim 10^6$–10^7 cm, $\mu \approx 1 \times 10^{28}\,{\rm G\,cm}^3$ (corresponding to a magnetic field of $\approx 2 \times 10^{10}$ G at the poles and assuming an $\dot{M}(R_{\rm M}) \approx 2 \times 10^{-8}\,{\rm M}_{\odot}\,{\rm yr}^{-1}$). The fact that the spherization radius and the magnetospheric radius are very close suggests that only the innermost portions of the accretion disc must be geometrically thick and generate a strong outflow. Such outflow might be responsible for the observed ADC, since it will surround the central X-ray source. The value of the magnetic field is somewhat smaller than the one inferred from the possible cyclotron line reported by Iaria et al. (2015), although it is of the same order of magnitude despite the large uncertainties involved. Indeed, we suggest the following:

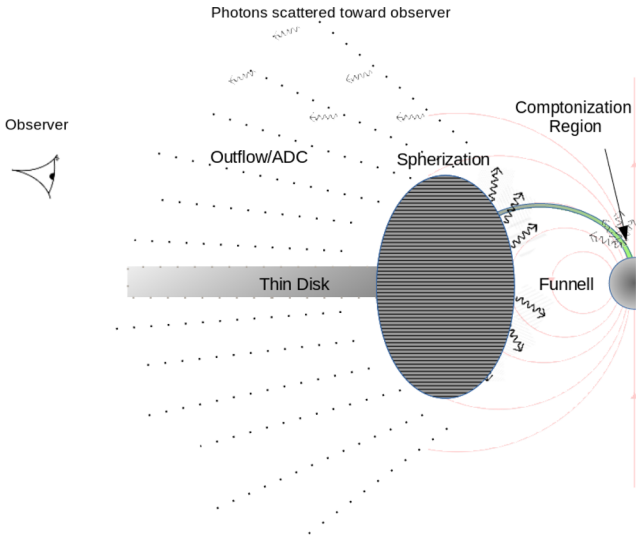

Figure 7. The illustrations show the geometry of the problem according to the super-Eddington scenario that we propose for 2A 1822−371 . The observer is located at an inclination angle $i = 82^{\circ}$ and we have chosen an aligned rotator for simplicity. The thick part of the accretion disc begins at the spherization radius and ends at the magnetospheric radius where the plasma becomes channelled towards the neutron star poles. The accretion flow along the magnetic field lines is abruptly stopped at the neutron star surface and a shock forms close to the neutron star surface. It is in this shock that the Comptonization process takes place. The outflow generates instead an optically thin cloud around the neutron star that is responsible for the scattering of a small portion of the X-ray photons towards the direction of the observer.

(i) The donor star of 2A 1822−371 is irradiated by a luminosity of $\approx 10^{36}\,{\rm erg\,s}^{-1}$.

(ii) The irradiation drives a thermal time-scale mass transfer of the order of $10^{-7}\,{\rm M}_{\odot}\,{\rm yr}^{-1}$.

(iii) The super-Eddington mass transfer rate generates an outflow at the spherization radius, very close to the magnetospheric radius.

(iv) The inner regions of the disc are geometrically thick and obscure the central source, as seen in Fig. 7.

Since the donor (and the observer) are nearly parallel to the accretion disc plane, even a very mild beaming will be sufficient to direct most of the radiation outside the line of sight of both the donor and the observer. Therefore, the donor will not be irradiated by an X-ray luminosity much larger than the observed $L_{\rm X} \approx 10^{36}\,{\rm erg\,s}^{-1}$.

Finally, as a self-consistency check, we need to verify whether the angular momentum loss due to the expulsion of material from the Roche lobe of the neutron star can alter significantly the orbit of the binary. As a limiting case, we assume that all the material transferred in the neutron star Roche lobe is expelled and thus, following Postnov & Yungelson (2006):

$$\frac{\dot{J}_{\rm orb}}{J_{\rm orb}} = \beta\frac{\dot{M}_2\,M_2}{M_{\rm NS}M_{\rm T}} \approx 10^{-16}\,{\rm s}^{-1}, \tag{10}$$

where $M_T = M_2 + M_{NS}$ is the total binary mass (assumed here to be approximately $2\,M_\odot$), J_{orb} and $\dot{J}_{orb}$ are the total orbital angular momentum of the binary and its variation, and β is the fraction of the mass that is expelled. By inserting this value in equation (7) and by considering that $\dot{M}_2 \approx 10^{-7}\,M_\odot\ yr^{-1}$, we see that the final value of $\dot{a}/a$ is still of the order of $10^{-14}\,s^{-1}$ that, again, is compatible with the observations.

4.4.1 *Possible tests of the proposed model*

If 2A 1822−371 is really a mildly super-Eddington source, then:

(i) The neutron star magnetic field must be of the order of a few times 10^{10} G.

(ii) The source should not show any torque reversal in the near future.

(iii) An outflow from the neutron star must be present and possible radio emission from a jet/outflow should be expected.

5 CONCLUSION

We examined 13 yr of data from *RXTE* and conclude that the long-term spin frequency derivative and the two phase-connected data sets, where we found short-term spin frequency derivatives, support an overall fast spin-up. The spin-up supports previous work by Iaria et al. (2015), Jain et al. (2010) and Chou et al. (2016). We tested if there was any flux–phase correlation present in this pulsar as there is in other systems, but found that there was no correlation.

We propose that the 2A 1822−371 is a relatively young binary (age of ∼1–10 Myr) in which the donor is in a thermal time-scale mass transfer phase. The orbital variation observed can be explained by the effect of the redistribution of angular momentum in the binary with no need for a large mass outflow from the donor star. An outflow is instead expected from the Roche lobe of the neutron star as a consequence of the nearly Eddington mass accretion rate occurring close to the neutron star magnetospheric radius. We propose that the outflow generates a large-scale optically thin corona with $\tau \approx 1$ that surrounds the system. The lack of variability in the fractional amplitude suggests, however, that the central source is always partially obscured and thus an optically thick region must form close to the neutron star at the approximate location of the spherization radius. We propose that this optically thick region generates a mild beaming as a consequence of the super-Eddington mass transfer rate. The Eddington/super-Eddington luminosity is not seen directly since the observer is viewing the source nearly edge-on, in a way similar to what happens in the black hole binary SS433 (King 2009).

ACKNOWLEDGEMENTS

The authors thank D. Giannios for use of the numerical code. AP acknowledges support from an NWO Vidi Fellowship. The authors also thank the referee, Rosario Iaria, for useful comments.

REFERENCES

Aly J. J., 1985, A&A, 143, 19
Bayless A. J., Robinson E. L., Hynes R. I., Ashcraft T. A., Cornell M. E., 2010, ApJ, 709, 251
Beri A., Jain C., Paul B., Raichur H., 2014, MNRAS, 439, 1940
Bhattacharya D., van den Heuvel E. P. J., 1991, Phys. Rep., 203, 1
Bildsten L. et al., 1997, ApJS, 113, 367
Bradt H. V., Rothschild R. E., Swank J. H., 1993, A&AS, 97, 355
Burderi L., Di Salvo T., Riggio A., Papitto A., Iaria R., D'Aì A., Menna M. T., 2010, A&A, 515, A44
Cavecchi Y. et al., 2011, ApJ, 740, L8
Chakrabarty D. et al., 1997, ApJ, 474, 414
Chou Y., Hsieh H.-E., Hu C.-P., Yang T.-C., Su Y.-H., 2016, ApJ, preprint (arXiv:1608.04190)
Cowley A. P., Schmidtke P. C., Hutchings J. B., Crampton D., 2003, AJ, 125, 2163
D'Angelo C. R., Spruit H. C., 2010, MNRAS, 406, 1208
D'Angelo C. R., Spruit H. C., 2012, MNRAS, 420, 416
D'Angelo C., Giannios D., Dullemond C., Spruit H., 2008, A&A, 488, 441
Frank J., King A., Raine D. J., 2002, Accretion Power in Astrophysics, 3rd edn. Cambridge Univ. Press, Cambridge
Ghosh P., Lamb F. K., 1979, ApJ, 234, 296
Giacconi R., Murray S., Gursky H., Kellogg E., Schreier E., Tananbaum H., 1972, ApJ, 178, 281
Giannios D., Spruit H. C., 2004, A&A, 427, 251
Goodson A. P., Winglee R. M., Böhm K.-H., 1997, ApJ, 489, 199
Griffiths R. E., Gursky H., Schwartz D. A., Schwarz J., Bradt H., Doxsey R. E., Charles P. A., Thorstensen J. R., 1978, Nature, 276, 247
Hakala P., Ramsay G., Muhli P., Charles P., Hannikainen D., Mukai K., Vilhu O., 2005, MNRAS, 356, 1133
Harlaftis E. T., Charles P. A., Horne K., 1997, MNRAS, 285, 673
Hartman J. M. et al., 2008, ApJ, 675, 1468
Haskell B., Patruno A., 2011, ApJ, 738, L14
Heinz S., Nowak M. A., 2001, MNRAS, 320, 249
Hellier C., Mason K. O., Smale A. P., Kilkenny D., 1990, MNRAS, 244, 39P
Iaria R., Di Salvo T., Burderi L., Robba N. R., 2001, ApJ, 557, 24
Iaria R., di Salvo T., Burderi L., D'Aí A., Papitto A., Riggio A., Robba N. R., 2011, A&A, 534, A85
Iaria R., Di Salvo T., D'Aì A., Burderi L., Mineo T., Riggio A., Papitto A., Robba N. R., 2013, A&A, 549, A33
Iaria R. et al., 2015, A&A, 577, A63
Jahoda K., Markwardt C. B., Radeva Y., Rots A. H., Stark M. J., Swank J. H., Strohmayer T. E., Zhang W., 2006, ApJS, 163, 401
Jain C., Paul B., Dutta A., 2010, MNRAS, 409, 755
Ji L., Schulz N. S., Nowak M. A., Canizares C. R., 2011, ApJ, 729, 102
Jonker P. G., van der Klis M., 2001, ApJ, 553, L43
Jonker P. G., van der Klis M., Groot P. J., 2003a, MNRAS, 339, 663
Jonker P. G., van der Klis M., Kouveliotou C., Méndez M., Lewin W. H. G., Belloni T., 2003b, MNRAS, 346, 684
King A. R., 2009, MNRAS, 393, L41
King A., Lasota J.-P., 2016, MNRAS, 458, L10
King A. R., Frank J., Kolb U., Ritter H., 1995, ApJ, 444, L37
King A. R., Frank J., Kolb U., Ritter H., 1996, ApJ, 467, 761
Lovelace R. V. E., Romanova M. M., Bisnovatyi-Kogan G. S., 1995, MNRAS, 275, 244
Maccarone T. J., Girard T. M., Casetti-Dinescu D. I., 2014, MNRAS, 440, 1626
Mason K. O., Cordova F. A., 1982, ApJ, 262, 253
Morris S. L., Liebert J., Stocke J. T., Gioia I. M., Schild R. E., Wolter A., 1990, ApJ, 365, 686
Muñoz-Darias T., Casares J., Martínez-Pais I. G., 2005, ApJ, 635, 502
Niu S., Yan S.-P., Lei S.-J., Nowak M. A., Schulz N. S., Ji L., 2016, Res. Astron. Astrophys., 16, 57
Papitto A., D'Aì A., Motta S., Riggio A., Burderi L., di Salvo T., Belloni T., Iaria R., 2011, A&A, 526, L3
Parmar A. N., Oosterbroek T., Del Sordo S., Segreto A., Santangelo A., Dal Fiume D., Orlandini M., 2000, A&A, 356, 175
Patruno A., Wijnands R., van der Klis M., 2009, ApJ, 698, L60
Patruno A., Hartman J. M., Wijnands R., Chakrabarty D., van der Klis M., 2010, ApJ, 717, 1253
Patruno A., Alpar M. A., van der Klis M., van den Heuvel E. P. J., 2012, ApJ, 752, 33
Podsiadlowski P., Rappaport S., Pfahl E. D., 2002, ApJ, 565, 1107
Postnov K. A., Yungelson L. R., 2006, Living Rev. Relativ., 9, 6

Sasano M., Makishima K., Sakurai S., Zhang Z., Enoto T., 2014, PASJ, 66, 35
Shakura N. I., Sunyaev R. A., 1973, A&A, 24, 337
Somero A., Hakala P., Muhli P., Charles P., Vilhu O., 2012, A&A, 539, A111
Tauris T. M., van den Heuvel E. P. J., 2006, Formation and Evolution of Compact Stellar X-ray Sources. Cambridge Univ. Press, Cambridge, p. 623
Ustyugova G. V., Koldoba A. V., Romanova M. M., Lovelace R. V. E., 2006, ApJ, 646, 304
van der Klis M., 2001, ApJ, 561, 943
van Straaten S., van der Klis M., Méndez M., 2003, ApJ, 596, 1155
White N. E., Holt S. S., 1982, ApJ, 257, 318
White N. E., Becker R. H., Boldt E. A., Holt S. S., Serlemitsos P. J., Swank J. H., 1981, ApJ, 247, 994
Yi I., Wheeler J. C., Vishniac E. T., 1997, ApJ, 481, L51

This paper has been typeset from a TEX/LATEX file prepared by the author.